Meteoritics 29, 334–348 (1994)

Basalt generation at the Apollo 12 site, Part 1: New data, classification, and re-evaluation

CLIVE R. NEAL[1], MATTHEW D. HACKER[1,2], GREGORY A. SNYDER[3], LAWRENCE A. TAYLOR[3], YUN-GANG LIU[4] AND ROMAN A. SCHMITT[4]

[1]Department of Civil Engineering and Geological Sciences, University of Notre Dame, Notre Dame, Indiana 46556, USA
[2]Department of Earth and Space Sciences, University of California, Los Angeles, California 90024, USA
[3]Department of Geological Sciences, University of Tennessee, Knoxville, Tennessee 37996, USA
[4]Department of Chemistry and Radiation Center, Oregon State University, Corvallis, Oregon 97331, USA

(Received 1993 April 13; accepted in revised form 1994 February 17)

Abstract–New data are reported from five previously unanalyzed Apollo 12 mare basalts that are incorporated into an evaluation of previous petrogenetic models and classification schemes for these basalts. This paper proposes a classification for Apollo 12 mare basalts on the basis of whole-rock Mg# [molar 100*(Mg/(Mg+Fe))] and Rb/Sr ratio (analyzed by isotope dilution), whereby the ilmenite, olivine, and pigeonite basalt groups are readily distinguished from each other. Scrutiny of the Apollo 12 feldspathic "suite" demonstrates that two of the three basalts previously assigned to this group (12031, 12038, 12072) can be reclassified: 12031 is a plagioclase-rich pigeonite basalt (Nyquist *et al.*, 1979); and 12072 is an olivine basalt. Only basalt 12038 stands out as a unique sample (Nyquist *et al.*, 1981) to the Apollo 12 site, but whether this represents a single sample from another flow at the Apollo 12 site or is exotic to this site is equivocal.

The question of whether the olivine and pigeonite basalt suites are co-magmatic is addressed by incompatible trace-element chemistry: the trends defined by these two suites when Co/Sm and Sm/Eu ratios are plotted against Rb/Sr ratio demonstrate that these two basaltic types cannot be co-magmatic. Crystal fractionation/accumulation paths have been calculated and show that neither the pigeonite, olivine, or ilmenite basalts are related by this process. Each suite requires a distinct and separate source region. This study also examines sample heterogeneity and the degree to which whole-rock analyses are representative, which is critical when petrogenetic interpretation is undertaken. Sample heterogeneity has been investigated petrographically (inhomogeneous mineral distribution) with consideration of duplicate analyses, and whether a specific sample (using average data) plots consistently upon a fractionation trend when a number of different compositional parameters are considered. Using these criteria, four basalts have been identified where reported analyses are *not* representative of the whole-rock composition: 12005, an ilmenite basalt; 12006 and 12036, olivine basalts; and 12031 previously classified as a feldspathic basalt, but reclassified as part of the pigeonite suite (Nyquist *et al.*, 1979).

INTRODUCTION

The Apollo 12 manned lunar mission returned a mare basalt suite which allows the only substantive look at basaltic volcanism on the western near-side of the Moon. The Apollo 14 mission also landed within this area, and mare basalts have been extensively studied from this site (Warner *et al.*, 1980; Dickinson *et al.*, 1985; Shervais *et al.*, 1985a; Neal *et al.*, 1988a), but these samples are predominantly clasts extracted from breccias and are on the order of milligrams, rather than grams as with the Apollo 12 mare samples. Although both suites are broadly classified as "Low-Ti", the Apollo 12 basalt suite contrasts compositionally with the high-alumina and VHK compositions found at Apollo 14 (Neal *et al.*, 1988b, 1989; Shervais *et al.*, 1985b), being relatively Al- and K-poor (Papike *et al.*, 1976; Papike and Vaniman, 1978; Neal and Taylor, 1992).

Many whole-rock analyses of the texturally and chemically diverse suite of Apollo 12 basalts were undertaken immediately after the return of this mission (*e.g.*, Biggar *et al.*, 1971; Bottino *et al.*, 1971; Brown *et al.*, 1971; Brunfelt *et al.*, 1971; Compston *et al.*, 1971; Ehmann and Morgan, 1971; Haskin *et al.*, 1971; Kushiro and Haramura, 1971; Maxwell and WIIK, 1971; Schnetzler and Philpotts, 1971; Wakita and Schmitt, 1971; Wänke *et al.*, 1971; Warner, 1971; and Willis *et al.*, 1971). Although initial studies (*e.g.*, LSPET, 1970; Kushiro and Haramura, 1971) recognized the importance of olivine fractionation in the petrogenesis of these basalts, further petrogenetic interpretation was not forthcoming at this time.

The Apollo 12 mare basalts were initially subdivided into three major types on the basis of petrography and major element chemistry (Table 1A): (1) olivine-pigeonite basalts; (2) ilmenite-bearing basalts; and (3) feldspathic basalts (James and Wright, 1972). Compositional variations within these groupings were ascribed to near-surface fractional crystallization processes (*e.g.*, Kushiro and Haramura, 1971; James and Wright, 1972). However, Compston *et al.* (1971) and Papanastassiou and Wasserburg (1971) suggested that the trace-element and isotopic variability within the olivine-pigeonite basalts were greater than expected by simple closed-system crystal fractionation. These observations, coupled with the work of Rhodes *et al.* (1977) led to the subdivision of the olivine-pigeonite grouping, forming a four-fold classification for the Apollo 12 mare basalts: (1) Olivine Basalts; (2) Pigeonite Basalts; (3) Ilmenite Basalts; and (4) Feldspathic Basalts (Table 1B). However, Rhodes *et al.* (1977) still maintained that the olivine and pigeonite basalts were co-magmatic, with the olivine basalts being made up essentially of crystal cumulates, and the pigeonite basalts

TABLE 1. Classifications of Apollo 12 basalts.

A. Petrographic Classification - James and Wright (1972)

Olivine-Pigeonite Basalts: 12002, 12004, 12008(?), 12009, 12011, 12012, 12014, 12017, 12018, 12019, 12020, 12021, 12035, 12036, 12040, 12052, 12053, 12055, 12057(?), 12065, 12075, 12076.

Ilmenite Basalts: 12022, 12031, 12039, 12045, 12046, 12047, 12051, 12056, 12057(?), 12062, 12063, 12064.

Feldspathic Basalts: 12006, 12038.

B. Whole-Rock Chemical Classification - Rhodes *et al.* (1977)*

Olivine Basalts: 12002, 12004, 12006, 12009, 12012, 12014, (12015), 12018, 12020, 12035, 12040, 12075, 12076.

Pigeonite Basalts: 12007, 12011, 12017, 12021, 12039, 12043, 12052, 12053, 12055, 12064, 12065.

Ilmenite Basalts: 12005, 12008, 12016, 12022, 12036(?), 12045, 12047, 12051, 12054, 12056, 12063.

Feldspathic Basalts: 12031(?), 12038, 12072@.

C. Whole-Rock Chemical Classification - This Study*

Olivine Basalts: 12002, 12004, 12006, 12009, 12012, 12014, 12015, 12018, 12020, 12035, 12036, 12040, 12072, 12075, 12076, 12077.

Pigeonite Basalts: 12007, 12011, 12017, 12019, 12021, 12031, 12039, 12043, 12052, 12053, 12055, 12065.

Ilmenite Basalts: 12005, 12008, 12016, 12022, 12045, 12046, 12047, 12051, 12054, 12056, 12061, 12062, 12063, 12064.

Feldspathic Basalt: 12038.

* = no analysis of 12057 available
@ = 12072 designated a feldspathic basalt by Beaty *et al.* (1979) and is included here for completeness.

representing the corresponding co-magmatic evolved liquid compositions. These authors also stated that the within group variations exhibited by these basalts are a result of olivine + minor Cr-spinel fractionation (with pigeonite replacing olivine in the pigeonite basalts) in flows up to 40 m thick, with the parental compositions for each basaltic type represented by the vitrophyres.

In a study of the olivine basalts, Walker *et al.* (1976a,b) studied the cumulate nature of the olivine basalts and the relative cooling rates exhibited by 12002. These authors noted that samples of the Apollo 12 olivine basalt suite exhibited a strong positive correlation of grain size with normative olivine content. This correlation was interpreted as resulting from settling of olivine in the basal portion of a cooling unit up to 30 m thick, thus identifying many of the olivine basalts as olivine cumulates.

The pigeonite suite is comprised of porphyritic basalts with a fine-grained groundmass and range continuously to coarse-grained microgabbros, with ophitic to graphic textures (Baldridge *et al.*, 1979). Although it was generally recognized that the pigeonite basalts were derived from the olivine basalts by crystal fractionation (James and Wright, 1972; Rhodes *et al.*, 1977), and Baldridge *et al.* (1979) stated that while the petrochemical and textural variations within the pigeonite suite are consistent with a co-magmatic origin with the olivine basalts, the compositional gap between these groups (Fig. 1) is difficult to reconcile with such a model. Eventually, Baldridge *et al.* (1979) concluded that these two basaltic groups were probably not co-magmatic on the basis of normative olivine differences between the finest-grained (parental) pigeonite (12011) and olivine (12015) basalts.

The ilmenite basalts exhibit a range of compositions which exceeds that defined by both the olivine and pigeonite basalts (Fig. 1). Dungan and Brown (1977) observed three textural categories of the Apollo 12 ilmenite basalts: (1) olivine porphyritic basalts; (2) medium-grained basalts with evolved compositions; and (3) coarse-grained olivine cumulates. These authors used vitrophyre 12008 as parental in their modelling of the ilmenite basalt compositions and concluded that most of the chemical variation within this suite can be accounted for by fractionation of olivine, equivalent to that in this vitrophyre. The range of compositions represents both crystal cumulate and evolved liquid compositions.

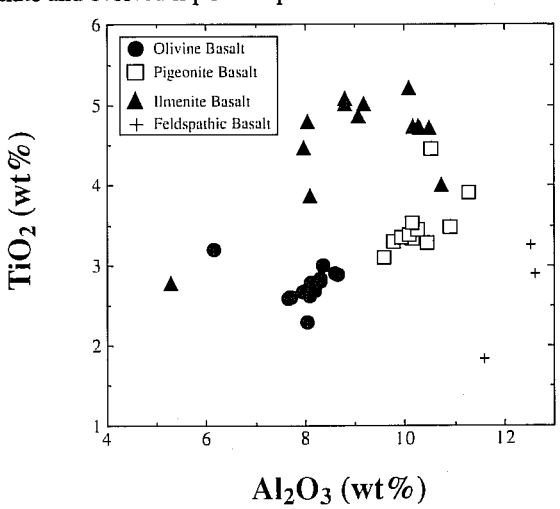

FIG. 1. Whole-rock compositions of Apollo 12 mare basalts represented on a TiO_2 (wt%) *vs.* Al_2O_3 (wt%) plot. Only old data have been plotted (see text for data sources). Note that the ilmenite basalts span the range of the olivine and pigeonite suites and, also, note the compositional gap between the olivine and pigeonite variants.

Only three basalts (12031, 12038, and 12072) were assigned to the feldspathic suite (*e.g.*, James and Wright, 1972; Beaty *et al.*, 1979). Beaty *et al.* (1979) argued for the presence of two types of feldspathic basalts on the basis of mineralogy, petrography, and whole-rock chemistry, with each group requiring a distinct source region. These authors concluded that 12031 could be derived from 12072 through fractionation of Cr-spinel, olivine, and pigeonite, which are the minerals forming the observed phenocryst assemblage. On the basis of Sr isotope compositions, Nyquist *et al.* (1979) demonstrated that 12031 was in fact a pigeonite basalt enriched in modal plagioclase. However, Beaty *et al.* (1979) insisted that bulk composition considerations indicate that none of the three feldspathic basalts (12031, 12038, and 12072) could have been derived by crystal fractionation from the Apollo 12 olivine, pigeonite, or ilmenite basalts. Isotopic evidence (Nyquist *et al.*, 1981) demonstrates that 12038 is clearly distinct from 12031, as well as from the olivine, pigeonite, and ilmenite basalts, consistent with the observations of Beaty *et al.* (1979).

This paper forms Part 1 of a two-part contribution and reports the petrography, mineral and whole-rock chemistry of five previously unanalyzed basalts (12019, 12046, 12061, 12062, 12077) and the modal mineralogy of all Apollo 12 mare basalts, in order to test the previous classifications. Also analyzed was basalt 12072, and we report the first whole-rock analysis of this sample, as the previous whole-rock major-element composition was a modal reconstruction (Beaty *et al.*, 1979). Furthermore, eight previously analyzed Apollo 12 mare basalts (12006, 12012, 12015, 12016, 12017, 12040, 12054, and 12076) were re-analyzed, primarily to obtain a full complement of trace-element data. These data are used to evaluate sample heterogeneity and to test previous petrogenetic models for the Apollo 12 mare basalts. The second part of this two-part contribution quantifies the petrogenesis of the Apollo 12 mare basalts, utilizing these new data and the conclusions of this paper (Neal *et al.*, 1994).

PETROGRAPHY AND MINERAL CHEMISTRY

The five "new" Apollo 12 mare basalt samples reported here have been classified using the petrographic and whole-rock chemical criteria developed by James and Wright (1972) and Rhodes *et al.* (1977). Sample 12019 is a pigeonite basalt, samples 12046, 12061, and 12062 are ilmenite basalts, and 12077 is an olivine basalt.

Detailed petrography and modal analyses (using a Swift point counter and a count population of 2500/ sample) were undertaken on these five previously unanalyzed Apollo 12 mare basalts, as well as 12072. The petrography of the six thin sections we wish to highlight is presented in Fig. 2 (a–f) and the Appendix. Generally, these six samples are fine- to medium-grained basalts which exhibit sub-ophitic to ophitic and variolitic textures. Phenocrysts of olivine and pyroxene are dominant, although no olivine is present in 12062,12, and microphenocrysts of chromite are present in 12072,3.

The mineral chemistry of each of the six samples is also summarized in the Appendix, and the pyroxene chemistry is highlighted in Fig. 3. Generally, the pyroxene phenocrysts are pigeonitic with zoning to subcalcic augite, whereas the groundmass pyroxenes generally trend to more Fe-rich compositions. Small rinds (< 0.1 mm wide) of Fe-rich pyroxene are occasionally found on phenocrysts. Pyroxene compositions either trend toward Ca-rich and then Fe-rich compositions (12019,5; 12046,6; and 12072,3) or

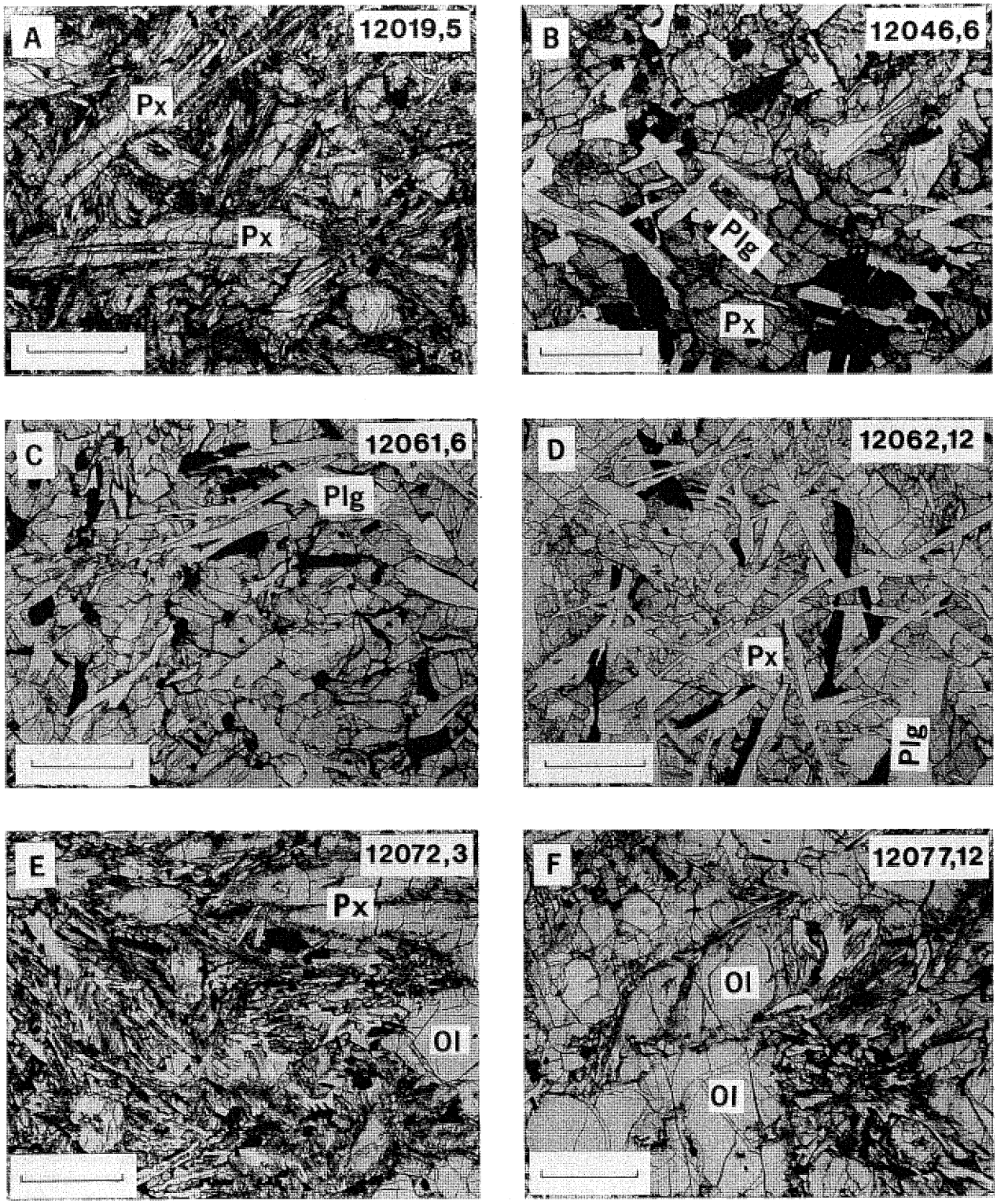

FIG. 2. Photomicrographs of the Apollo 12 mare basalts. Scale bar in each case represents 0.5 mm. (a) 12019,5–Pigeonite basalt containing pyroxene phenocrysts set in a ophitic to variolitic groundmass; (b) 12046,6–Ilmenite basalt with ophitic to sub-ophitic texture; (c) 120061,6–Ilmenite basalt with ophitic to sub-ophitic texture; (d) 12062,12–Ilmenite basalt with sub-ophitic texture; (e) 12072,3–Olivine basalt with large olivine phenocrysts set is a variolitic to plagioclase poikilitic groundmass; (f) 12077,12–Olivine basalt with large olivine phenocrysts sets in a sub-ophitic to variolitic groundmass.

exhibit compositions trending from pigeonite to subcalcic augite or from pigeonite to more Fe-rich compositions (12061,6; 12077,12). TiO_2 and Al_2O_3 contents increase and then decrease from core-to-rim in pyroxenes from 12019,5, 12046,6, and 12072,3, whereas in 12061,6 and 12077,12 Al_2O_3 and TiO_2 exhibit a core-to-rim increase. A core-to-rim decrease in all cases is exhibited by Cr_2O_3. These relations are probably controlled by plagioclase, ulvöspinel, and chromite crystallization (*e.g.*, Bence and Papike, 1972).

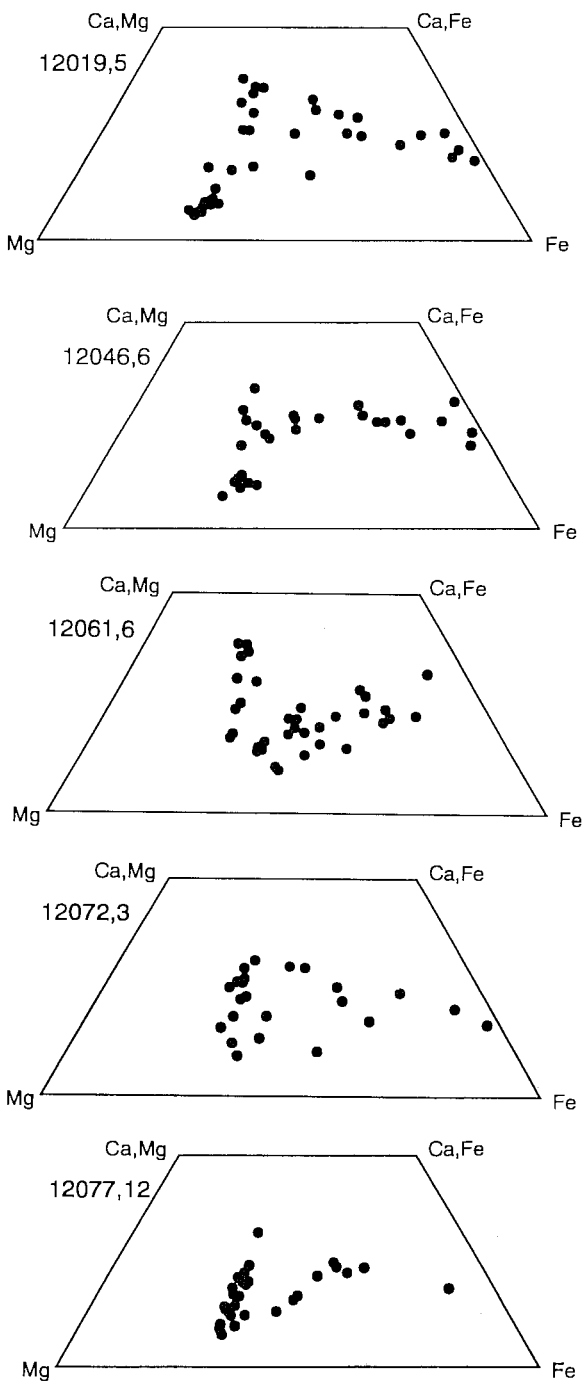

FIG. 3. Pyroxene quadrilaterals for four of the five previously unanalyzed Apollo 12 mare basalts and 12072. Only four of the new basalts are represented, as the thin section for 12062 contained a thin section.

Where present, olivine exhibits zonation from relatively Fo-rich cores towards more Fa-rich rims. This is especially pronounced where olivine forms the cores to pyroxenes. Plagioclase also exhibits core-to-rim zonation in each basalt analyzed, becoming slightly more Ab- and FeO-rich with a parallel decrease in An contents. Ilmenite exhibits no core-to-rim zonation, containing < 2 wt% MgO, but with slight variation between grains. Likewise, ulvöspinel contains < 2 wt% MgO (except in 12077,12 where it contains up to 11 wt% MgO), but does exhibit zonation toward Mg-poor, Ti-rich compositions. Finally, chromites within these basalts exhibit variable compositions, zoning toward ulvöspinel compositions.

The analyzed FeNi metal grains of the five basalts studied petrographically contain high Co contents (1.0–2.6 wt%) for a given Ni concentration (1.2–8.2 wt%), typical of Apollo 12 basalts (Goldstein and Yackowitz, 1971) (Fig. 4).

CLASSIFICATION

The modes of all Apollo 12 mare basalt samples have been determined using a Swift point counter; results are presented in Table 2 and correspond to a population of 2500 counts/sample. This was conducted in order to demonstrate the convenient groupings of these samples on the basis of modal mineralogy. Broad correlations between the modes and basaltic type can be seen from Table 2. For example, the broad petrographic subdivisions of olivine, pigeonite, and ilmenite basalts are apparent (pigeonite basalts are olivine-poor and olivine basalts are olivine-rich, whereas the ilmenite basalts are relatively enriched in ilmenite). However, the modal pyroxene abundances overlap in the olivine and pigeonite basalts, as do the modal ilmenite abundances in the ilmenite suite with those from both the pigeonite and olivine subdivisions. Furthermore, the feldspathic basalts are not overly distinguished by plagioclase contents, at least not from the thin sections we analyzed. We conclude that while generalities can be made using modal data, such data are not sufficient to allow a classification of Apollo 12 mare basalts, even though the number of analyzed samples has grown. This observation is why we favor a classification based upon whole-rock chemistry, similar to that of Rhodes *et al.* (1977) (Table 1B), but using different parameters, resulting in the classification given in Table 1C.

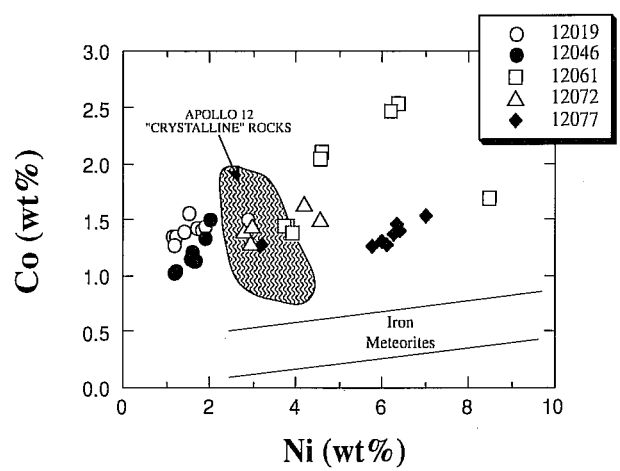

FIG. 4. The Fe,Ni metal compositions from four of the five new Apollo 12 mare basalts + 12072 containing elevated Co abundances relative to other Apollo 12 mare basalts (Goldstein and Yakowitz, 1971).

We propose a classification for the Apollo 12 basalts based upon Mg# [molar Mg/(Mg+Fe)*100] and Rb/Sr ratio (Fig. 5; Table 1C). Olivine basalts contain a Mg# greater than 46 and a Rb/Sr ratio greater than 0.008; pigeonite basalts contain a Mg# lower than 46 but a Rb/Sr ratio greater than 0.008; and ilmenite basalts have a Mg# which spans both the olivine and pigeonite suites but a Rb/Sr ratio less than 0.008 (Fig. 5). These parameters were chosen because: (1) they conveniently split the basalts into the olivine, pigeonite, and ilmenite divisions; (2) allow an idea of magmatic evolution (Mg#); and (3) represent a possible gauge of source composition and/or degree of partial melting (Rb/Sr; see the companion paper, Neal *et al.*, 1994). Note that only basalts which have had Rb and Sr abundances determined by isotope dilution have been plotted, resulting in the omission of several Apollo 12 basalts from this diagram. These can be classified according to other chemical similarities with basalts included in Fig. 5. This proposed classification does not readily separate the feldspathic basalts (on the basis of Mg# and Rb/Sr ratio, the feldspathic basalts overlap with the ilmenite basalts). However, as we will demonstrate, the feldspathic group is in reality comprised of only one sample, 12038.

WHOLE-ROCK CHEMISTRY

Splits of 14 Apollo 12 mare basalts were analyzed by INAA techniques at Oregon State University. The analytical procedure used is similar to that for which details have been documented by Hughes *et al.* (1989). As noted earlier, five previously unanalyzed basalts (12019, 12046, 12061, 12062, 12077) were targeted by our study, as well as eight basalts which had only partial analyses conducted upon them (12006, 12012, 12015, 12016, 12017, 12040, 12054, 12076). Beaty *et al.* (1979) reported a whole-rock major-element composition of 12072 calculated by modal reconstruction,

TABLE 2. Modal mineralogy of the Apollo 12 mare basalts. Classification as in Table 1C.

Sample No.	Olivine	Undiff. Px	Plag.	SiO_2	Glass/Meso.	Ilm	Usp	Chr	Tr	FeNi	Undiff. Opqs.
Olivine Basalts											
12002	22.2	41.1	27.9	0.0	2.3	0.9	1.8	2.3	0.2	1.3	
12004	17.8	43.4	30.5	0.0	1.8	1.4	1.7	2.0	0.3	1.0	
12006	22.6	28.7	43.4	0.0	0.5	1.1	1.2	2.2	0.1	0.2	
12009	48.8	0.0	0.1	0.0	47.2	1.2	0.3	1.9	0.0	0.5	
12012	21.6	53.5	19.0	0.2	1.6	1.9	0.6	0.7	0.4	0.5	
12014	24.8	46.7	24.5	0.0	2.6	0.6	0.2	0.5	0.0	0.1	
12015	62.3	0.0	0.0	0.0	33.7	0.0	0.4	2.8	0.4	0.4	
12018	22.6	60.1	10.9	0.4	2.5	0.5	0.7	1.3	0.3	0.7	
12020	19.0	51.2	25.9	0.0	0.5	0.2	0.7	2.0	0.1	0.4	
12035	21.4	51.1	24.3	0.0	0.6	0.1	0.2	2.1	0.1	0.1	
12036*	24.0	58.0	12.0	0.0	0.0	--	--	--	--	--	5.0
12040	22.7	51.5	21.6	0.1	0.3	2.3	0.0	1.2	0.2	0.0	
12072	5.7	49.0	38.9	3.1	1.4	1.2	0.0	0.2	0.3	0.1	
12075	15.7	57.5	21.7	0.0	1.6	0.6	0.4	2.3	0.1	0.1	
12076	26.2	46.8	14.4	0.1	3.7	4.0	1.0	3.0	0.4	0.4	
12077#	16.6	61.7	19.3	0.0	0.7	0.4	0.0	1.1	0.1	0.1	
Pigeonite Basalts											
12007	0.0	48.2	39.8	7.3	0.4	4.0	0.1	0.0	0.2	0.0	
12011	7.6	52.9	30.6	3.4	1.4	2.9	0.1	0.5	0.5	0.1	
12017	4.0	61.2	25.0	0.5	6.3	1.5	0.3	0.7	0.4	0.1	
12019#	2.5	58.3	31.9	2.8	0.3	3.7	0.1	0.2	0.1	0.1	
12021	1.0	71.3	25.5	0.2	0.0	1.2	0.0	0.5	0.1	0.2	
12031	0.0	49.2	40.2	4.9	0.9	3.9	0.1	0.0	0.7	0.1	
12039	0.0	55.0	39.5	0.5	0.5	2.8	0.1	1.4	0.1	0.1	
12043	0.9	57.7	32.9	3.7	0.8	3.5	0.1	0.1	0.2	0.0	
12052	1.0	57.9	31.7	0.0	3.0	3.5	0.4	2.1	0.3	0.1	
12053	0.0	67.1	21.1	0.2	4.6	3.9	0.3	1.3	1.1	0.4	
12055	1.0	58.2	33.8	0.4	1.4	0.4	0.6	2.7	1.4	0.1	
12065	0.3	68.6	24.9	0.5	2.1	1.6	0.6	1.0	0.2	0.2	
Ilmenite Basalts											
12005	30.0	56.5	11.0	0.0	0.1	1.9	0.5	0.0	0.0	0.0	
12008	38.2	20.4	2.0	0.0	33.9	4.7	0.0	0.6	0.0	0.2	
12016	12.0	52.1	29.1	0.0	0.6	4.8	1.6	0.0	0.0	0.0	
12022	19.5	56.0	12.2	0.2	2.3	6.3	0.7	2.1	0.3	0.4	
12045*	8.8	57.0	20.6	0.6	5.7	--	--	--	--	--	7.3
12046#	0.8	60.1	29.9	1.1	2.1	3.4	1.0	1.0	0.4	0.2	
12047	0.0	48.4	38.0	5.3	2.0	5.3	1.0	0.0	0.0	0.0	
12051	0.0	60.4	30.7	0.3	1.2	5.3	0.3	1.1	0.3	0.4	
12054	10.8	62.1	27.9	0.1	1.9	5.2	0.5	1.9	0.3	0.1	
12056	10.8	49.2	28.8	0.8	2.5	6.8	1.6	0.0	0.0	0.0	
12061#	0.2	64.6	24.8	0.5	2.5	4.2	0.9	1.9	0.2	0.2	
12062#	0.0	57.0	32.2	1.4	3.5	0.3	1.6	3.6	0.2	0.2	
12063	2.8	64.6	21.6	0.1	2.5	4.6	1.5	1.9	0.3	0.1	
12064	0.0	55.4	39.1	0.0	0.9	3.9	0.0	0.6	0.1	0.0	
Feldspathic Basalt											
12038	0.1	48.8	43.8	2.7	0.7	3.5	0.1	0.1	0.1	0.1	

Undiff. Px. = Undifferentiated Pyroxenes; Plag. = Plagioclase; Meso = Mesostasis; Ilm = Ilmenite; Usp = Ulvöspinel; Chr = Chromite; Tr = Troilite; FeNi = FeNi Metal; Undiff. Opqs = Undifferentiated Opaques; # = "New" Apollo 12 mare basalt; * = cover slip on thin section.

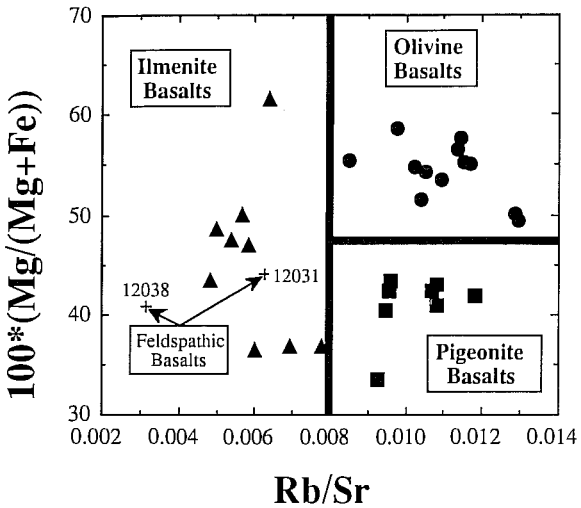

FIG. 5. Classification of Apollo 12 mare basalt on the basis of molar 100*(Mg/(Mg+Fe)) *vs.* Rb/Sr ratio. All Rb and Sr data are by isotope dilution (Nyquist *et al.*, 1977, 1979, 1981; Murthy *et al.*, 1971; Papanastassiou and Wasserburg, 1970, 1971).

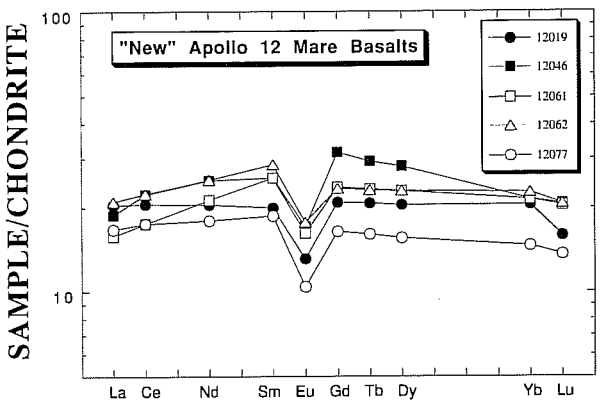

FIG. 6. Chondrite-normalized rare-earth-element (REE) profiles of the five new Apollo 12 mare basalts. The Gd data are projected from Yb through Tb.

but until this study (analysis of 12072,8), no actual analysis of this sample had been conducted. With these new analyses (Table 3), we have obtained a full complement of trace-element data in order to evaluate previous petrogenetic models for the Apollo 12 mare basalts.

"New" Apollo 12 Basalts (12019, 12046, 12061, 12062, 12077)

The five "new" Apollo 12 mare basalts are somewhat variable in composition (Table 3), consistent with our earlier designation of these into the ilmenite (12046, 12061, 12062), olivine (12077), and pigeonite (12019) basalt suites. The variation in major elements practically spans the range defined by previously analyzed Apollo 12 mare basalts. The Mg# exhibits a range of 39.2 (12046,17) to 56.9 (12077,1). Using the general mare basalt classification proposed by Neal and Taylor (1992), these new samples are part of the Low-Ti/Low-Al/Low-K suite: TiO_2 contents are below 6 wt% (2.6–5.0 wt%); Al_2O_3 contents are below 11 wt% (7.7–10.5 wt%); and K_2O contents are well below 2000 ppm (415–523 ppm) (Table 3). The compatible trace elements show moderate variation, especially in Cr (2006–5056 ppm), but the high field-strength elements (Hf, Th, Ta) have similar abundances (2.5–3.9 ppm, 0.56–0.79 ppm, and 0.45–0.56 ppm, respectively; Table 3). The rare-earth-element (REE) profiles are generally LREE-depleted [$(La/Sm)_N$ = 0.62–0.90], although the LREE profiles of 12019,13 [$(La/Sm)_N$ = 0.90] and 12077,1 [$(La/Sm)_N$ = 0.89] appear to be flat in Fig. 6. All samples have negative Eu anomalies [$(Sm/Eu)_N$ = 1.49–1.80] and exhibit a slight decrease in abundance (relative to chondrites) from Tb to Lu (Fig. 6).

Analyses of 12006, 12012, 12015, 12016, 12017, 12040, 12054, 12072 and 12076.

Original analyses of these samples have been reported by Compston *et al.* (1971), Scoon (1971), Rhodes *et al.* (1977), and Nyquist *et al.* (1979). The new analyses were conducted to obtain a full complement of trace-element data, as well as being a check on whether the reported data are representative of whole-rock compositions. Our new analyses are similar (within the analytical uncertainties) to those previously published (Table 3 and Fig. 7) with the following exceptions:

12006,16 (Rhodes *et al.*, 1977) contains lower K_2O, Sc, Sr, Ba, Hf, and REE abundances than ,5 (this study) (Fig. 7a), although both are LREE-enriched and possess negative Eu anomalies [$(Sm/Eu)_N$ = 1.99 and 1.52, respectively]. The TiO_2, Al_2O_3, CaO, and Na_2O contents are slightly higher in our new analysis (12006,5) and MgO, Cr, and Co contents are slightly lower.

12016,25 (this study) contains higher MgO, Al_2O_3, and Ni, with lower K_2O, Sr, Hf, and REE abundances than ,9 (Rhodes *et al.*, 1977). The REE profiles are parallel (Fig. 7d), but the abundance difference is probably due to the more primitive/cumulate nature of the new analysis (higher olivine contents; Dungan and Brown, 1977), witnessed by increased MgO and Ni (Table 3).

12054,61 (this study) contains higher MgO and lower CaO abundances than the analysis of 12054,62 (Rhodes *et al.*, 1977). This may be explained by variations in olivine and plagioclase in the two samples analyzed.

12072,8 (this study) represents the first whole-rock analysis of this sample. The major-element abundances are totally dissimilar to the modally reconstructed analysis of Beaty *et al.* (1979) (Table 3). The REE profile is similar to other Apollo 12 Low-Ti/Low-Al/Low-K basalts (Fig. 7f).

DISCUSSION

Sample Heterogeneity

While the new and duplicate analyses have undoubtedly expanded the Apollo 12 data base, they have highlighted problems of sampling errors which must be addressed before any petrogenetic interpretation can occur. To conserve lunar samples, many principal investigators were allocated ≤0.2 g aliquants of Apollo 11 and Apollo 12 mare basalts, thereby resulting in sampling errors which were not appreciated during the early Apollo research activities. Three criteria are used to identify sample heterogeneity: (1) Inhomogeneous mineral distribution as seen in thin section; (2) Discrepancies between several whole-rock analyses; and (3) Inconsistencies in plotting averaged data on fractionation trends using several compositional criteria.

Petrographic Heterogeneity–We have identified heterogeneity in the distribution of plagioclase and/or ilmenite and/or

olivine in thin sections of 12005, 12006, 12016, 12036, 12054, and 12072. The general textures of the heterogeneous samples are: 12005, 12006, 12016, 12036, and 12054 = medium- to coarse-grained sub-ophitic to ophitic with inhomogeneous olivine, plagioclase, and/or ilmenite/ulvöspinel distribution; 12072 = fine- to medium-grained variolitic with inhomogeneous olivine (as phenocrysts), plagioclase, and ilmenite distribution. Neal *et al.* (1992a,b) erroneously reported that 12015 was heterogeneous, suggesting that vitrophyres could not be used as prospective parents. This is corrected here as the new analysis of 12015 is reported as approximately the same as that reported by Rhodes *et al.* (1977) (Fig. 7c).

Chemical Heterogeneity–Another approach which identifies unrepresentative whole-rock analyses is to use the variation in several whole-rock analyses of a given basalt, if the sample has been analyzed more than once. The criterion we used to designate representative from unrepresentative was that variation between individual analyses for a given basalt did not exceed the variation exhibited by the suite in which the basalt was classified (this being the coherent field represented by averaged data). Although petrographic heterogeneity was noted in 12005, 12036, and 12072, only one analysis each has been reported. We will assume that these single analyses are representative of the whole-rock composition, although until duplicate analyses have been conducted, petrogenetic interpretation using these samples must proceed with caution.

In addition to those basalts exhibiting mineralogical heterogeneity noted above, variations between duplicate analyses of 12002, 12006, 12016, 12021, 12052, 12054, and 12063 were noted. In order to demonstrate the nature of such heterogeneity, duplicate analyses of 12002, 12052, and 12063 are plotted in Fig. 8 (a–c), where major- and trace-element data have been normalized to a Bulk Moon composition (Taylor, 1982, 1993). A linear scale is used to exaggerate the similarities or differences in composition between the various analyses. Generally, major-element compositions are similar, except for TiO_2 contents, consistent with heterogeneous ilmenite/ulvöspinel distribution within this basalt. However, the greatest variation is in the incompatible trace-element abundances, especially K and the REE. This variation can be accounted for by incorporating various proportions of incompatible-element-rich mesostasis (*cf.*, Lindstrom and Haskin, 1978, 1981; Haskin and Korotev, 1977). Such discrepancies can be semi-quantified by assuming a KREEP basalt composition for the mesostasis and calculating how much is to be added to the analysis

TABLE 3. Whole-rock chemistry of Apollo 12 basalts analyzed during this study. Comparisons are made with previously reported analyses of the same basalt where applicable.

	NEW	1	NEW	1	NEW	1	2	NEW	1	NEW	1		NEW	NEW	3
	12006 ,5	12006 ,16	12012 ,23	12012 ,18	12015 ,23	12015 ,9-11	12015 ,23	12016 ,25	12016 ,9	12017 ,50	12017 ,36	12019 ,13*	12040 ,187	12040	
wt (g)	0.238		0.0604		0.548			0.666		0.561		0.670	0.654		
SiO_2 (wt%)		44.23		44.17		44.98			42.78		47.27			44.08	
TiO_2	3.2	2.59	2.7	2.64	2.9	2.86		3.5	4.02	3.3	3.37	3.0	2.6	2.41	
Al_2O_3	10.6	7.67	8.1	7.71	8.7	8.57		8.2	7.23	9.6	10.0	9.6	7.8	7.18	
FeO	20.8	20.94	21.4	20.69	20.5	20.18		22.2	22.64	20.1	19.72	20.61	20.9	21.27	
MnO	0.258	0.29	0.262	0.30	0.269	0.29		0.252	0.30	0.271	0.29	0.252	0.255	0.28	
MgO	12.8	14.67	16.0	14.37	12.3	11.88		15.1	12.65	8.7	7.63	9.2	17.1	16.21	
CaO	9.8	8.13	8.0	8.47	8.9	9.21		8.2	8.42	10.1	10.97	9.1	6.9	8.1	
Na_2O	0.409	0.20	0.207	0.21	0.239	0.23		0.258	0.22	0.267	0.27	0.253	0.199	0.19	
K_2O	0.075	0.05	0.052	0.06	0.06	0.06		0.049	0.06	0.071	0.09	0.053	0.039	0.04	
Sc (ppm)	47.2	40.1	44.0	41.9	48.4	46.1		49.0	49.4	53.9	52.8	53.0	42.6		
V	172		186		186			153		183		177	166	153	
Cr	3890	6250	4260	4780	4250	4653		3790	3950	3510	3550	3670	4140	3760	
Co	45.2	60	57.7	56	47.8	51		54.3	54	38.8	32	41.5	59.5	52	
Ni	70	110	43	60	62	50		78	25	38		30	101	40	
Sr	104	89	143	89	84	94	102	85	126	103	118	130	94	80.6	
Ba	117	56	104	56	65	61	63.7	---	59	95	75	71	54	40	
La	9.0		5.3		6.2		6.23	4.3		7.0		6.7	4.3		
Ce	26.3	15.7	15.3	13.8	16.0	16.3	16.8	12.7	16.2	23.4		19.1	13.5		
Nd	19.6		10.8		14.4		12.8	7.0		13.2		12.9	8.8		
Sm	5.7	3.77	3.6	4.02	4.3	4.31	4.32	4.1	5.5	4.8	5.1	4.6	3.1		
Eu	1.42	0.72	0.8	0.76	0.98	0.81	0.91	1.04	1.06	1.00		1.01	0.79		
Gd							5.86								
Tb	1.35	1.02	0.86	1.17	1.16	1.05		1.13	1.42	1.24		1.20	0.92		
Dy	8.1		4.9		7.4		7.03	5.5		7.7		7.0	5.2		
Yb	4.1	3.3	3.0	3.4	3.6	3.7	3.55	3.6	5.0	4.2	4.4	4.5	2.9		
Lu	0.59	0.47	0.46	0.47	0.52	0.53	0.514	0.53	0.67	0.57	0.66	0.54	0.37		
Y		31		33		35			45					22	
Zr		97		99		110			117					5.7	
Nb		6.4		6.6		6.6			6.1					2	
Hf	3.8	3.0	2.6	3.4	3.3	3.5		3.0	6.3	3.4		3.2	2.4		
Ta	0.56		0.37		0.38			0.26		0.48		0.56	0.30		
Th	0.74		0.67		0.74			0.47		0.87		0.79	0.47		

* = "New" Apollo 12 Basalts; 1 = Rhodes *et al.* (1977); 2 = Nyquist *et al.* (1979); 3 = Compston *et al.* (1971); 4 = Scoon (1971); 5 = Beaty *et al.* (1979).

with the least abundant incompatible trace elements in order to generate that with the most. Mass balance calculations were undertaken using KREEP basalt 15386 (Vaniman and Papike, 1980) as representative of the mesostasis material in mare basalts. Results indicate that the discrepancies between the analyses of the basalts depicted in Fig. 8 are accounted for by incorporation/omission of 1–5% KREEP-like mesostasis material. This produces variations in the incompatible trace elements, but not the compatible trace and major elements. Variations that do occur in major-element oxide abundances can generally be accounted for by heterogeneous mineral distribution within the sample. Also plotted is an example of sample homogeneity, where six analyses of 12075 exhibit little variation (Fig. 8d).

Plotting Consistency–While a certain basalt may display heterogeneity between duplicate analyses, the average of these data may still fall upon a fractionation trend (*i.e.*, the average of all the disparate analyses gives a "representative" whole-rock composition). Therefore, in conjunction with the use of duplicate analyses, we have also evaluated whether a sample, represented as an average of duplicate analyses, where possible, plots consistently on an apparent fractionation trend using a number of different compositional parameters. If averages of the basalts exhibiting heterogeneity between duplicate analyses plot consistently on their respective fractionation trends, they were cautiously included in this evaluation of Apollo 12 mare basalt petrogenesis. Basalts which have only one analysis reported have also been evaluated with respect to plotting consistency. This approach allows each basalt to be represented as a single data point and has identified four basalt whole-rock compositions which appear to be inhomogeneous: 12005, an ilmenite basalt; 12006 and 12036, olivine basalts; and 12031, a feldspathic basalt.

This study of sample heterogeneity suggests that although petrographic heterogeneity is observed, reported whole-rock analyses maybe be similar (and vice versa). Furthermore, while different whole-rock analyses exhibit variations, averaged data can be representative of the whole-rock composition. Using the criteria outlined above, analyses of four basalts are considered unrepresentative of whole-rock composition–12005, 12006, 12031, and 12036.

The Feldspathic Basalts

The inclusion of 12031 in the feldspathic suite was seriously undermined by the work of Nyquist *et al.* (1979). On the basis of initial Sr ratios, Nyquist *et al.* (1979) concluded that 12031 was in

TABLE 3: Continued.

	4	NEW	NEW	1	NEW	NEW	NEW	5	NEW	1	NEW	Uncertainties#
	12040 ,36	12046 ,17*	12054 ,61	12054 ,62	12061 ,3*	12062 ,22*	12072 ,8	12072	12076 ,42	12076 ,18	12077 ,10*	(%)
wt (g)		0.547	0.694		0.560	0.617	0.618		0.561		0.620	
SiO_2 (wt%)	43.89			45.86				48.14		44.87		
TiO_2	2.74	4.6	4.7	4.63	4.9	4.6	3.0	1.81	2.8	2.76	2.5	10-30
Al_2O_3	7.41	10.5	10.1	10.5	8.8	10.3	8.5	11.64	8.5	8.1	7.7	<5
FeO	20.83	20.2	20.2	19.51	21.9	20.7	21.3	17.46	21.2	20.66	21.2	<2
MnO	0.26	0.259	0.262	0.29	0.274	0.266	0.262	0.25	0.257	0.30	0.267	<2
MgO	16.1	7.3	7.7	6.76	11.6	8.1	13.3	8.57	14.6	12.26	15.7	5-15
CaO	7.87	10.6	10.0	11.93	9.1	9.9	8.7	11.38	9.0	9.03	7.7	5-10
Na_2O	0.20	0.293	0.294	0.31	0.276	0.297	0.227	0.37	0.222	0.21	0.202	<2
K_2O	0.04	0.063	0.062	0.07	0.057	0.060	0.059	0.04	0.056	0.06	0.050	10-30
Sc (ppm)		60.2	64.3	64	60.8	59.1	47.1		47.2	46.4	41.4	<2
V		138	144		158	140	165		167		197	10-20
Cr		2010	2150	2300	3210	2120	3760		4130	4640	5050	<5
Co		31.0	33.7	31	45.8	32.7	50.5		54.0	54	59.5	<5
Ni		----	31		48	----	54		73		125	5-25
Sr		158	111	162	149	180	----		94	94	----	10-20
Ba		72	76	64	----	69	56		70	59	----	10-25
La		6.2	6.3		5.2	6.9	6.2		5.9		5.5	<5
Ce		19.3	18.7	18.8	15.1	20.2	17.7		17.5		15.1	2-15
Nd		15.8	16.0		13.4	14.6	11.6		11.4		9.0	5-15
Sm		5.2	5.5	6.0	5.2	5.8	4.2		4.0	4.03	3.8	<5
Eu		1.32	1.4	1.27	1.25	1.36	0.96		0.92		0.80	2-10
Gd												
Tb		1.70	1.48	1.85	1.35	1.34	1.07		1.08		0.93	5-15
Dy		8.8	9.4		8.1	8.8	6.6		7.0		5.8	5-10
Yb		4.7	4.9	5.8	4.7	5.0	3.6		3.3	3.4	3.2	2-10
Lu		0.70	0.75	0.78	0.69	0.70	0.50		0.49	0.51	0.46	2-10
Y				51								
Zr				128								
Nb				6.3								
Hf		3.7	4.1	4.8	3.6	3.9	3.0		3.2		2.5	2-10
Ta		0.49	0.40		0.49	0.45	0.43		0.53		0.45	5-10
Th		0.67	0.61		0.56	0.77	0.77		0.90		0.65	2-10

* = "New" Apollo 12 Basalts; # = for the uncertainty ranges, the larger numbers correspond to the uncertainties attached to the NEW 12012,23 values for a small sample mass.

fact a plagioclase-rich pigeonite basalt. Furthermore, on the basis of Rb/Sr ratio and Mg#, 12031 falls within the ilmenite suite (Fig. 5) and also falls off the pigeonite trend in Fig. 9a,b, consistent with our conclusion that the reported whole-rock analysis is not representative of the bulk composition.

The inclusion of 12072 in the feldspathic suite is negated by our analysis of 12072,8. In Fig. 9a,b, the new analysis of 12072 moves it into the olivine basalt field. As the original major-element composition reported by Beaty *et al.* (1979) was a modal reconstruction, we strongly suggest reclassification of this sample as part of the Apollo 12 olivine suite. Therefore, we use only our INAA data for 12072,8 when representing this sample. This reclassification of 12072 as an olivine basalt reduces the population of the feldspathic "suite" to only one member, 12038. Nyquist *et al.* (1981) reported the unique isotopic signature of this basalt which may show either that 12038: (1) represents an exotic sample placed at the Apollo 12 site as part of impact ejecta; or (2) is the only returned sample of the feldspathic suite, with feldspathic basalt flow(s) present in the Ocean of Storms.

The Olivine and Pigeonite Basalts

The original petrogenetic model describing the olivine and pigeonite basalt suites as being co-magmatic is investigated using the new data. In some plots, the new pigeonite basalt (12019) falls within the pigeonite field (Fig. 9a), yet in others, it plots within the olivine field (Fig. 9b). Is this an intermediate sample? Furthermore, one of the analyses of the heterogeneous olivine basalt 12006 plots within the compositional gap between the

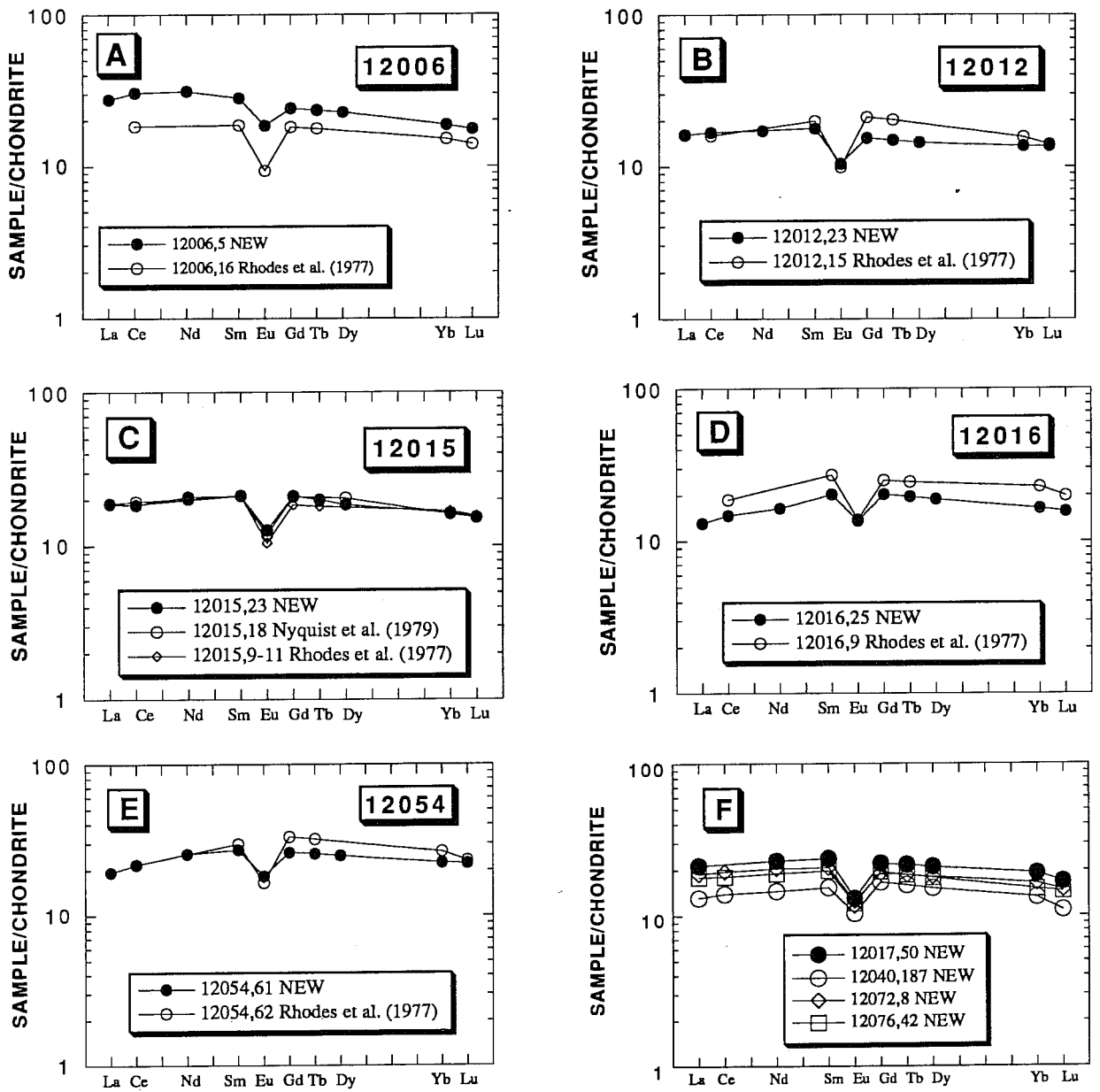

FIG. 7. Chondrite-normalized REE profiles comparing our new data with that previously published for the following Apollo 12 mare basalts: (a) 12006; (b) 12012; (c) 12015; (d) 12016; (e) 12054; and (f) complete REE profiles analyzed by this work for previously analyzed basalts without a full complement of the REE. The Gd data are projected from Yb through Tb.

olivine and pigeonite suites (Fig. 9a,b), tending to add support to the conclusion of James and Wright (1972) that these two suites are related by crystal fractionation. In order to test this, we have used vitrophyric samples as parental compositions and generated crystal fractionation/accumulation paths for the olivine, pigeonite and ilmenite basalts (Fig. 10a,b). The fractionating assemblage for each parent was derived from the MAGFOX program of Longhi (1991). This resulted in the following fractionating sequences: *pigeonite basalts* = 0–1% = olivine (100); 1–5% = olivine (80) + chromite-ulvöspinel (20); 5–15% = pigeonite (98) + chromite-ulvöspinel (2); 15–30% = pigeonite (33) + plagioclase (67); *olivine basalts* = 0–1% = 0livine (100); 1–23% = olivine (94) + chromite-ulvöspinel (6); 23–30% = pigeonite (100); and *ilmenite basalts* = 0–1% = olivine (100); 1–27% = olivine (94) + chromite-ulvöspinel (6); 28–30% = clinopyroxene (42) + plagioclase (58). While Longhi (1987) pointed out the limits of this program to model chromite crystallization, its incorporation here allows a first approximation. As such, Cr has not been used in petrogenetic modelling (Neal *et al.*, 1994). The models do not exceed 30% because the major-element trends defined by each of these three suites are generated by this amount of crystal fractionation/accumulation (Neal and Taylor, 1993a,b; Neal *et al.*, 1994). Partition coefficients were taken from the compilation reported by Snyder *et al.* (1992).

The Rb/Sr ratio (all data by isotope dilution) is plotted against Co/Sm (Fig. 10a) and Sm/Eu (Fig. 10b), with the modelled crystal fractionation/accumulation paths indicated. It is evident that the pigeonite basalts cannot be the evolved equivalents of the olivine basalts, whether the olivine parent or the pigeonite parent is used (Fig. 10 a,b). Furthermore, neither the olivine or the pigeonite basalts are related to the ilmenite basalt suite by crystal fractionation/accumulation. In Fig. 10b, the model paths are shorter for the ilmenite basalts because plagioclase is required as a fractionating phase in order to alter Sm/Eu and Rb/Sr ratios. For the ilmenite basalt parent, plagioclase only becomes a liquidus phase after 27% crystallization. For the olivine basalt parent, plagioclase is not a liquidus phase, so Rb/Sr and Sm/Eu ratios do not change. Therefore, the model crystal fractionation/accumulation paths plot directly on top of the parental composition.

We conclude that: (1) short-range unmixing is not responsible for the compositional variations observed in the Apollo 12 mare basalt suites; and (2) the Apollo 12 olivine and pigeonite basalts are not related, each being derived from a separate and distinct source region.

SUMMARY

This study of Apollo 12 mare basalts has produced the following conclusions. (1) Five "new" samples of Apollo 12 mare

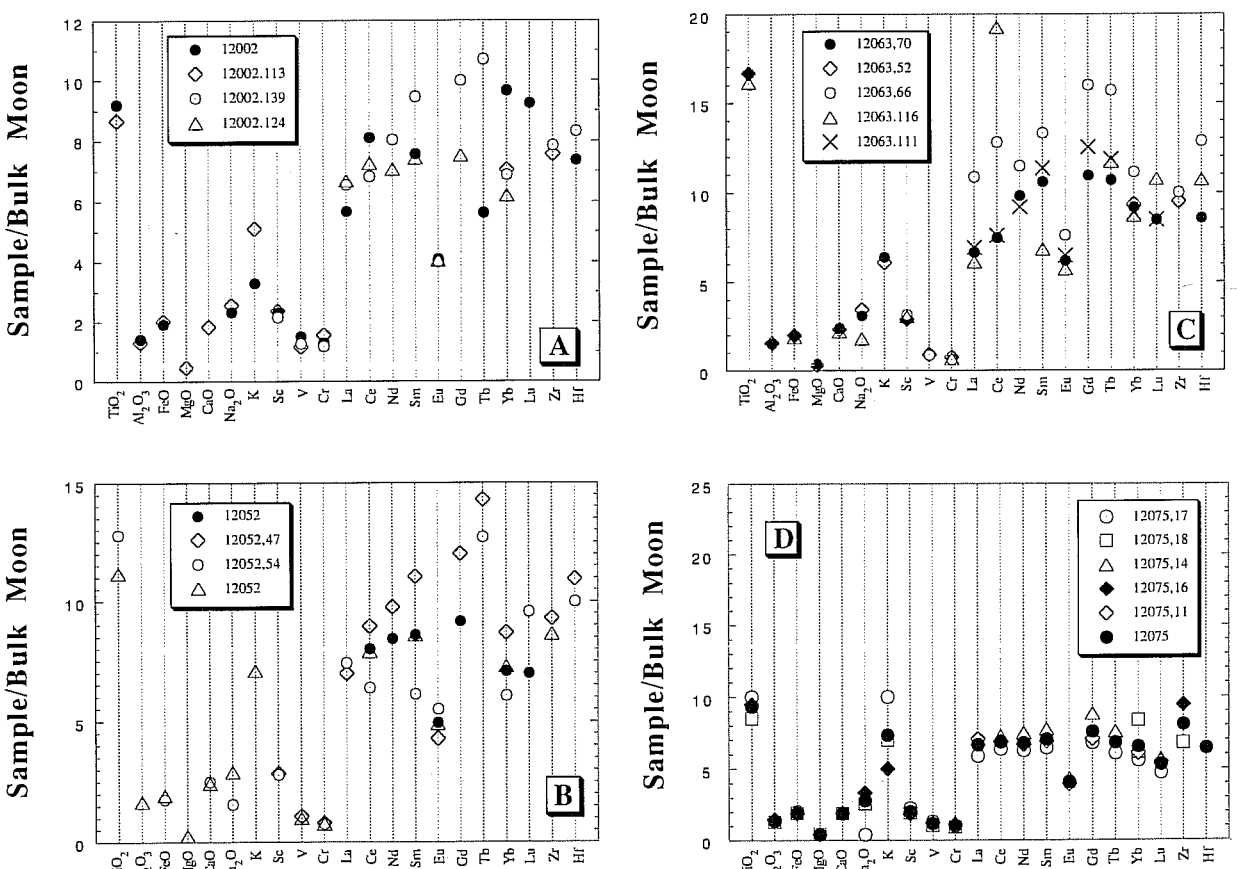

FIG. 8. Bulk Moon normalized major- and trace-element plots for basalts exhibiting petrographic and/or chemical heterogeneity (12002, 12052, 12063; a through c) and an example of chemical homogeneity (12075; d). A linear scale is used in order to exaggerate the similarities or differences between different whole-rock analyses of the same basalt. Data from Brunfelt *et al.* (1971); Hubbard and Gast (1971); Taylor *et al.* (1971); Willis *et al.* (1971); Schnetzler and Philpotts (1971); Kharka and Turekian (1971); Compston *et al.* (1971); Wakita and Schmitt (1971); Cuttitta *et al.* (1971); Haskin *et al.*, 1971); Engel *et al.* (1971). Normalizing values from Taylor (1982, 1993).

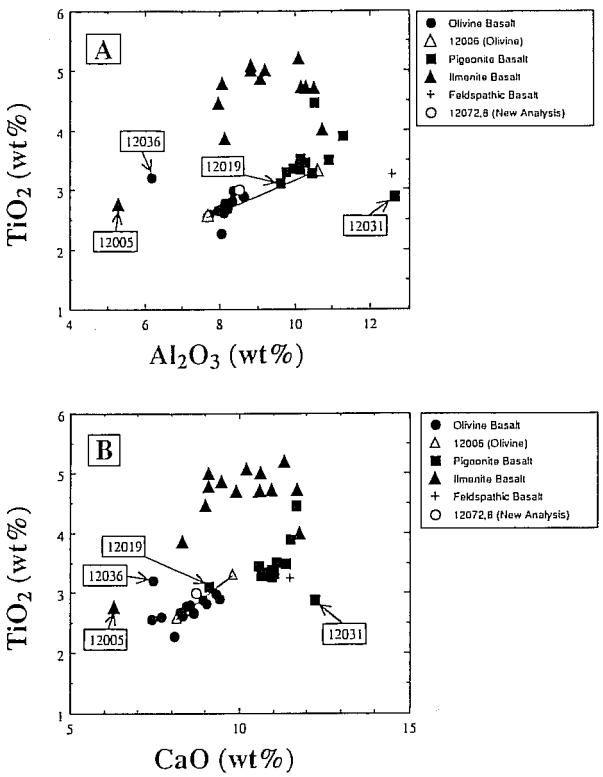

FIG. 9. Whole-rock compositions of Apollo 12 mare basalts incorporating the new data reported here on plots of: (a) TiO_2 (wt%) *vs.* Al_2O_3 (wt%); and (b) TiO_2 (wt%) *vs.* CaO (wt%). Note the variation in 12072 and 12006 and where 12019 plots in each diagram.

basalts are made up of three ilmenite basalts, one olivine basalt, and one pigeonite basalt. (2) The classification of Apollo 12 mare basalts on the basis of modal mineralogy cannot be used to readily distinguish between all Apollo 12 basalts from the current data base. We propose that a whole-rock chemical classification of Mg# *vs.* Rb/Sr be used. (3) A study of sample heterogeneity (both petrographic and chemical) has highlighted basalts 12005, 12006, 12031, and 12036 as having whole-rock analyses which are not representative of their bulk composition. (4) Original feldspathic basalt 12072 is reclassified as part of the olivine suite with the feldspathic suite represented by only one sample, 12038. (5) The compositional ranges observed in each of the Apollo 12 mare basalt suites is not generated by addition/subtraction (filter-pressing) of a KREEP-like mesostasis fluid just prior to total solidification. (6) The pigeonite and olivine suites are not related by crystal fractionation/accumulation and were derived from distinct and separate sources.

These conclusions are used in the second part of this two part contribution to model the petrogenesis of olivine, pigeonite, and ilmenite suites.

Acknowledgements–Many thanks to Allan Patchen for microprobe analyses. A detailed review by Scott Hughes and thought-provoking comments from an anonymous reviewer greatly improved this manuscript. This study has been supported through NASA grant NAG 9-415 to L.A.T., a Notre Dame *Jesse H. Jones* Research Fellowship to C.R.N. and M.D.H., and NASA grant NAG 9-63 to R.A.S.

Editorial handling: P. Warren

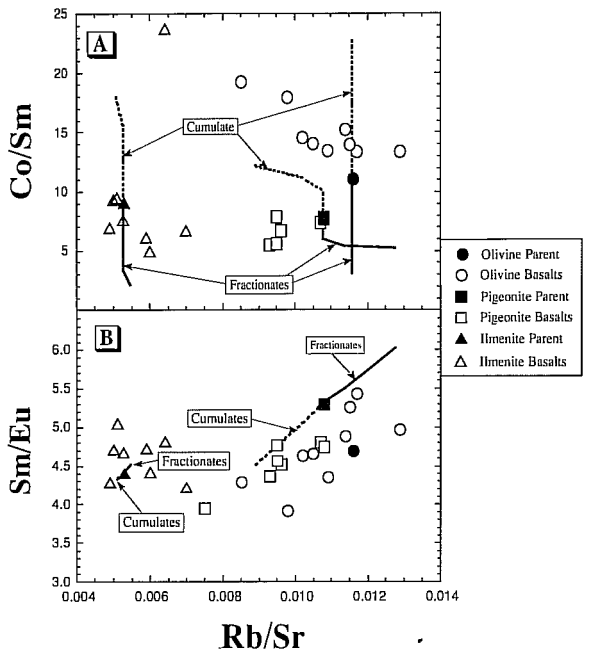

FIG. 10. The Co/Sm and Sm/Eu ratios plotted against Rb/Sr ratio for all Apollo 12 mare basalts. The Rb/Sr ratio is analyzed by isotope dilution. Superimposed on these plots are the crystal fractionation/accumulation paths derived from the MAGFOX program of Longhi (1991). The model paths each extend to 30% crystal fractionation/accumulation, in conjunction with major element modelling (Neal *et al.*, 1994) This figure demonstrates that the olivine and pigeonite suites are unrelated by crystal fractionation/accumulation. Vitrophyres (parental compositions) within each of the groups are identified.

REFERENCES

BALDRIDGE W. S., BEATY D. W., HILL S.M.R. AND ALBEE A. L. (1979) The petrology of the Apollo 12 pigeonite basalt suite. *Proc. Lunar Planet. Sci. Conf.* **10th,** 141–179.

BEATY D. W., HILL S. M. R., ALBEE A. L. AND BALDRIDGE W. S. (1979) Apollo 12 feldspathic basalts 12031, 12038, and 12072: Petrology, comparison, and interpretation. *Proc. Lunar Planet. Sci. Conf.* **10th,** 115–139.

BENCE A. E. AND PAPIKE J. J. (1972) Pyroxenes as recorders of lunar basalt petrogenesis: Chemical trends due to crystal-liquid interactions. *Proc. Lunar Planet. Sci. Conf.* **3rd,** 431–469.

BIGGAR G. M., O'HARA M. J., PECKETT A. AND HUMPHRIES D. J. (1971) Lunar lavas and the achondrites: Petrogenesis of protohypersthene basalts in the maria lava lakes. *Proc. Lunar Planet. Sci. Conf.* **2nd,** 617–643.

BOTTINO M. L., FULLAGAR P. D., SCHNETZLER C. C. AND PHILPOTTS J. A. (1971) Sr isotopic measurements in Apollo 12 samples. *Proc. Lunar Planet. Sci. Conf.* **2nd,** 1487–1491.

BROWN G. M., EMELEUS C. H., HOLLAND J. G., PECKETT A. AND PHILLIPS R. (1971) Picrite basalts, ferrobasalts, feldspathic norites, and rhyolites in a strongly fractionated lunar crust. *Proc. Lunar Planet. Sci. Conf.* **2nd,** 583–600.

BRUNFELT A. O., HEIER K. S. AND STEINNES E. (1971) Determination of 40 elements in Apollo 12 materials by neutron activation analysis. *Proc. Lunar Planet. Sci. Conf.* **2nd,** 1281–1290.

COMPSTON W., BERRY H., VERNON M. J., CHAPPELL B. W. AND KAYE M. J. (1971) Rubidium-strontium chronology and chemistry of lunar material from the Ocean of Storms. *Proc. Lunar Planet. Sci. Conf.* **2nd,** 1471–1485.

CUTTITTA F., ROSE H. J., JR., ANNELL C. S., CARRON M. K., CHRISTIAN R. P., DWORNIK E. J., GREENLAND L. P., HELZ A. P. AND LIGON D. T., JR. (1971) Elemental composition of some Apollo 12 lunar rocks and soils. *Proc. Lunar Planet. Sci. Conf.* **2nd,** 1217–1229.

DICKINSON T., TAYLOR G. J., KEIL K., SCHMITT R. A., HUGHES S. S. AND SMITH M. R. (1985) Apollo 14 aluminous mare basalts and their possible relationship to KREEP. *Proc. Lunar Planet. Sci. Conf.* **15th,** *Jour. Geophys. Res.* **90,** C365–C374.

DUNGAN M. A. AND BROWN R. W (1977) The petrology of the Apollo 12 ilmenite basalt suite. *Proc. Lunar Planet. Sci. Conf.* **8th,** 1339–1381.

EHMANN W. D. AND MORGAN J. W. (1971) Major element abundances in

Apollo 12 rocks and fines by 14 MeV neutron activation. *Proc. Lunar Planet. Sci. Conf.* **2nd,** 1237–1245.

ENGEL A. E. J., ENGEL C. G. SUITON A. L. AND MYERS A. T. (1971) Composition of five Apollo 11 and Apollo 12 rocks and one Apollo 11 soil and some petrogenetic considerations. *Proc. Lunar Sci. Conf.* **2nd,** 439–448

GOLDSTEIN J. I. AND YAKOWITZ H. (1971) Metallic inclusions and metal particles in the Apollo 12 lunar soils. *Proc. Lunar Planet. Sci. Conf.* **2nd,** 177–191.

HASKIN L. A. AND KOROTEV R. L. (1977) Test for a model for trace element partition during closed-system solidification of a silicate liquid. *Geochim. Cosmochim. Acta* **41,** 921–939.

HASKIN L. A., HELMKE P. A., ALLEN R. O., ANDERSON M. R., KOROTEV R. L. AND ZWEIFEL K. A. (1971) Rare-earth elements in Apollo 12 lunar materials. *Proc. Lunar Planet. Sci. Conf.* **2nd,** 1307–1317.

HUBBARD N. J. AND GAST P. W. (1971) Chemical composition and origin of nonmare lunar basalts. *Proc. Lunar Sci. Conf.* **2nd,** 999–1020

HUGHES S. S., DELANO J. W. AND SCHMITT R. A. (1989) Petrogenetic modelling of 74220 high-Ti orange volcanic glasses and the Apollo 11 and 17 high-Ti mare basalts. *Proc. Lunar Planet. Sci. Conf.* **19th,** 175–188.

JAMES O. B. AND WRIGHT T. L. (1972) Apollo 11 and 12 mare basalts and gabbros: Classification, compositional variations, and possible petrogenetic relations. *Bull. Geol. Soc. Am.* **83,** 2357–2382.

KHARKAR D. P. AND TUREKIAN K. K. (1971) Analyses of Apollo 11 and Apollo 12 rocks and soils by neutron activation. *Proc. Lunar Planet. Sci. Conf.* **2nd,** 1301–1305.

KUSHIRO I. AND HARAMURA H. (1971) Major element variation and possible source materials of Apollo 12 crystalline rocks. *Science* **171,** 1235–1237.

LSPET (Lunar Sample Preliminary Examination Team) (1970) Preliminary examination of the lunar samples from Apollo 12. *Science* **167,** 1325–1339.

LINDSTROM M. M. AND HASKIN L. A. (1978) Causes of compositional variations within mare basalt suites. *Proc. Lunar Planet. Sci. Conf.* **9th,** 465–486.

LINDSTROM M. M. AND HASKIN L. A. (1981) Compositional inhomogeneities in a single Icelandic tholeiite flow. *Geochim. Cosmochim. Acta* **45,** 15–31.

LONGHI J. (1987) On the connection between mare basalts and picritic volcanic glasses. *Proc. Lunar Planet. Sci. Conf.* **17th,** *J. Geophys. Res.* **92,** E349–E360.

LONGHI J. (1991) Comparative liquidus equilibria of hypersthene-normative basalts at low pressure. *Amer. Mineral.* **76,** 785–800.

MAXWELL J. A. AND WIIK H. B. (1971) Chemical composition of Apollo 12 lunar samples 12004, 12033, 12051, 12052, and 12065. *Earth Planet. Sci. Lett.* **10,** 285–288.

MURTHY V. R., EVENSEN N. M., JAHN B. M. AND COSCIO M. R., JR. (1971) Rb-Sr ages and elemental abundances of K, Rb, Sr, and Ba in samples from the Ocean of Storms. *Geochim. Cosmochim. Acta* **35,** 1139–1153.

NEAL C. R. AND TAYLOR L. A. (1992) Petrogenesis of mare basalts: A record of lunar volcanism. *Geochim. Cosmochim. Acta* **56,** 2177–2211.

NEAL C. R. AND TAYLOR L. A. (1993a) Petrogenesis of Apollo 12 mare basalts, part 1: Multiple melts and fractional crystallization to explain olivine and ilmenite basalt compositions (abstract). *Lunar Planet. Sci.* **24,** 1057–1058.

NEAL C. R. AND TAYLOR L. A. (1993b) Petrogenesis of Apollo 12 mare basalts, part 2: An open system model to explain the pigeonite basalt compositions (abstract). *Lunar Planet. Sci.* **24,** 1059–1060.

NEAL C. R., TAYLOR L. A. AND LINDSTROM M. M. (1988a) Apollo 14 mare basalt petrogenesis: Assimilation of KREEP-like components by a fractionating magma. *Proc. Lunar Planet. Sci. Conf.* **18th,** 139–153.

NEAL C. R., TAYLOR L. A. AND LINDSTROM M. M. (1988b) The importance of lunar granite and KREEP in very high potassium (VHK) basalt petrogenesis. *Proc. Lunar Planet. Sci. Conf.* **18th,** 121–137.

NEAL C. R., TAYLOR L. A., SCHMITT R. A., HUGHES S. S. AND LINDSTROM M. M. (1989) High-alumina (HA) and very high potassium (VHK) basalt clasts from Apollo 14 breccia, part 2 - whole rock geochemistry: Further evidence for combined assimilation and fractional crystallization within the lunar crust. *Proc. Lunar Planet. Sci. Conf.* **19th,** 147–161.

NEAL C. R., HACKER M. D., TAYLOR L. A., SCHMITT R. A. AND LIU Y.-G. (1992a) The petrogenesis of Apollo 12 mare basalts, part 1: The "lumpers" versus the "splitters" (abstract). *Lunar Planet. Sci.* **23,** 975–976. .

NEAL C. R., HACKER M. D., TAYLOR L. A., SCHMITT R. A. AND LIU Y.-G. (1992b) The petrogenesis of Apollo 12 mare basalts, part 2: Identification of distinct olivine and pigeonite suites, and open-system evolution (abstract). *Lunar Planet. Sci.* **23,** 977–978.

NEAL C. R., HACKER M. D., TAYLOR L. A., SCHMITT R. A. AND LIU Y.-G. (1994) Basalt generation at the Apollo 12 site, Part 2: Source heterogeneity, multiple melts, and crustal contamination. *Meteoritics* **29,** 349–361.

NYQUIST L. E., BANSAL B. M., WOODEN J. L. AND WIESMANN H. (1977) Sr-isotopic constraints on the petrogenesis of Apollo 12 mare basalts. *Proc. Lunar Sci. Conf.* **8th,** 1383–1415.

NYQUIST L. E., SHIH C.-Y., WOODEN J .L., BANSAL B. M. AND WIESMANN H. (1979) The Sr and Nd isotopic record of Apollo 12 basalts: Implications for lunar geochemical evolution. *Proc. Lunar Planet. Sci. Conf.* **10th,** 77–114.

NYQUIST L. E., WOODEN J. L., SHIH C.-Y., WIESMANN H. AND BANSAL B. M. (1981) Isotopic and REE studies of lunar basalt 12038: Implications for petrogenesis of aluminous mare basalts. *Earth Planet. Sci. Lett.* **55,** 335–355.

PAPANASTASSIOU D. A. AND WASSERBURG G. J. (1970) Rb-Sr ages from the Ocean of Storms. *Earth Planet. Sci. Lett.* **8,** 269–278.

PAPANASTASSIOU D. A. AND WASSERBURG G. J. (1971) Lunar chronology and evolution from Rb-Sr studies of Apollo 11 and 12 samples. *Earth Planet. Sci. Lett.* **11,** 37–62.

PAPIKE J. J. AND VANIMAN D. T. (1978) Luna 24 ferrobasalts and the mare basalt suite: Comparative chemistry, mineralogy, and petrology. In *Mare Crisium: The View from Luna 24* (eds.R. B. Merrill and J. J. Papike), pp. 371–401. Pergamon Press, New York.

PAPIKE J. J., HODGES F. N., BENCE A. E., CAMERON M. AND RHODES J. M. (1976) Mare basalts: Crystal chemistry, mineralogy, and petrology. *Rev. Geophys. Space Phys.* **14,** 475–540.

RHODES J. M., BLANCHARD D. P., DUNGAN M. A., BRANNON J. C. AND RODGERS K. V. (1977) Chemistry of Apollo 12 mare basalts: Magma types and fractionation processes. *Proc. Lunar Planet. Sci. Conf.* **8th,** 1305–1338.

SCHNETZLER C. C. AND PHILPOTTS J. A. (1971) Alkali, alkaline earth, and rare-earth element concentrations in some Apollo 12 soils, rocks, and separated phases. *Proc. Lunar Planet. Sci. Conf.* **2nd,** 1101–1122.

SCOON J. H. (1971) Chemical analyses of lunar samples 12040 and 12064. *Proc. Lunar Sci. Conf.* **2nd,** 1259–1260.

SHERVAIS J. W., TAYLOR L. A. AND LINDSTROM M. M. (1985a) Apollo 14 mare basalts: Petrology and geochemistry of clasts from consortium breccia 14321. *Proc. Lunar Planet. Sci. Conf.* **15th,** *J. Geophys. Res.* **90,** C375–C395.

SHERVAIS J. W., TAYLOR L. A., LAUL J. C., SHIH C.-Y. AND NYQUIST L. E. (1985b) Very high potassium (VHK) basalts: Complications in mare basalt petrogenesis. *Proc. Lunar Planet. Sci. Conf.* **16th,** *J. Geophys. Res.* **90,** D3–D18.

SNYDER G. A., TAYLOR L. A. AND NEAL C. R. (1992) A chemical model for generating the sources of mare basalts: Imperfect, geologically realistic fraactional crystallization of the lunar magmasphere. *Geochim. Cosmochim. Acta* **56,** 3809–3823.

TAYLOR S. R. (1982) *Planetary Science: A Lunar Perspective.* The Lunar and Planetary Institute, Houston, Texas. 481 pp.

TAYLOR S. R. (1993) *Solar System Evolution: A New Perspective.* The Lunar and Planetary Institute, Houston, Texas. 307 pp.

TAYLOR S. R., RODOWSKI R., MUIR P., GRAHAM A. AND KAYE M. (1971) Trace element chemistry of lunar samples from the Ocean of Storms. *Proc. Lunar Planet. Sci. Conf.* **2nd,** 1083–1099.

VANIMAN D. T. AND PAPIKE J. J. (1980) Lunar highland melt rocks: Chemistry, petrology and silicate mineralogy. *Proc. Conf. Lunar Highlands,* 271–338.

WAKITA H. AND SCHMITT R. A. (1971) Bulk elemental composition of Apollo 12 samples: Five igneous and one breccia rock and four soils. *Proc. Lunar Planet. Sci. Conf.* **2nd,** 1231–1236.

WALKER D., LONGHI J., KIRKPATRICK R. J. AND HAYS J. F. (1976a) Differentiation of an Apollo 12 picrite magma. *Proc. Lunar Planet. Sci. Conf.* **7th,** 1365–1389.

WALKER D., KIRKPATRICK R. J., LONGHI J. AND HAYS J. F. (1976b) Crystallization history of lunar picritic basalt sample 12002: Phase-equilibria and cooling-rate studies. *Geol. Soc. Am. Bull.* **87,** 646–656.

WÄNKE H., WLOTZKA F., BADDENHAUSEN H., BALACESCU A., SPETTEL B., JAGOUTZ E., KRUSE H., QUIJANO-RICO M. AND RIEDER R. (1971) Apollo 12 samples: Chemical composition and its relation to sample locations and exposure ages, the two component origin of the various soil samples and studies on lunar metallic particles. *Proc. Lunar Planet. Sci. Conf.* **2nd,** 1187–1208.

WARNER J. L. (1971) Lunar crystalline rocks: Petrology and geology. *Proc. Lunar Planet. Sci. Conf.* **2nd,** 469–480.

WARNER R. D., TAYLOR G. J., KEIL K., MA M.-S. AND SCHMITT R. A. (1980) Aluminous mare basalts: New data from Apollo 14 coarse-fines. *Proc. Lunar Planet. Sci. Conf.* **11th,** 87–104.

WILLIS J. P., AHRENS L. H., DANCHIN R. V., ERLANK A. J., GURNEY J. J., HOFMEYR P. K., MCCARTHY T. S. AND ORREN M. J. (1971) Some inter-element relationships between lunar rocks and fines, and stony meteorites. *Proc. Lunar Planet. Sci. Conf.* **2nd,** 1123–1138.

APPENDIX
Petrography and Mineral Chemistry Summary

12019,5 (Fig. 2a)

MINERAL	MORPHOLOGY	RELATIONSHIP	SIZE (MM)	COMPOSITION	SPECIAL FEATURES
Olivine	Anhedral/Embayed	Corroded Phenos.	≤0.7	Cores = Fo_{88}	20 μm rim of oliv. + glass on pheoncrysts and
		Cores to Px	≤0.2	Rims = Fo_{53}	0.1 mm Chromite inclusions
Pyroxenes	Subhedral/Anhedral	Phenocrysts	≤2.0	$Wo_6En_{38}Fs_{28}$	20 μm rim of Px + glass on pheocrysts and
		Groundmass	≤0.3	$Wo_{36}En_{38}Fs_{26}$	0.1 mm Chromite inclusions
				$Wo_{18}En_2Fs_{80}$	
Plagioclase	Laths	Groundmass	≤0.6	Cores = $An_{91-93}Ab_{9-7}$	Skeletal with rounded glass inclusions
				Rims = $An_{88}An_{12}$	
Tridymnite	Anhedral/Mesostasis	Groundmass	≤0.05	---	"Crinkled" Texture
Glass	Interstitial	Groundmass	≤0.05	SiO_2 = 96-98 wt%	Opaque
				Al_2O_3 = 0.6-1.2 wt%	
				FeO = 0.6-1.7 wt%	
				$K_2O \approx 0.2$ wt%	
Ilmenite	Subhedral	Groundmass	≤1.0	MgO = 0.5 wt%	Sawtooth Margins. Contains rounded glass blebs (<0.02 mm). Poikilitically encloses other groundmass minerals
Ulvöspinel	Anhderal	Groundmass	<0.2	MgO ≈ 1 wt%	Also found as rims on Chromite inclusions in Oliv. and Px
				Mg# = 29-32	
				Cr/(Cr+Al) = 0.73-0.74	
Chromite	Euhedral	Incluions in Oliv. and Px	≤0.6	MgO = 6-7 wt%	Contain Ulvöspinel rims
				Mg# = 29-32	
				Cr/(Cr+Al) = 73-74	
Troilite	Anhedral	Groundmass	≤0.05	---	Usually associated with ilmenite, occasionally discrete
FeNi Metal	Anhedral	Groundmass	≤0.05	Co = 1.3-1.6 wt%	Discrete grains or as blebs in troilite
				Ni = 1.2-2.9 wt%	

12046,6 (Fig. 2b)

MINERAL	MORPHOLOGY	RELATIONSHIP	SIZE (MM)	COMPOSITION	SPECIAL FEATURES
Olivine	Anhedral/Embayed	Cores to Px Phenos.	≤0.4	Not Analyzed	
Pyroxene	Subhedral/Embayed	Phenocrysts	≤2.0	$Wo_8En_{63}Fs_{29}$	Simple twinning on {100}
	Subhedral	Groundmass	0.4-0.8	$Wo_{29}En_{48}Fs_{23}$	Groundmass often associated with mesostasis
				$Wo_{20}En_5Fs_{75}$	
Plagioclase	Subhedral	Groundmass Laths	≤1.5	Cores = $An_{91-93}Ab_{9-7}$	Occasional 0.01 mm glass inclusions
				Rims = $An_{87-88}Ab_{13-12}$	
Tridymite	Anhedral	Groundmass	≤0.2	---	"Crinkled" Texture
Glass	Interstitial	Groundmass	≤0.2	SiO_2 = 98-99 wt%	Opaque
				FeO = 0.2-0.4 wt%	
				Al_2O_3 = 0.5-0.6 wt%	
				$K_2O \approx 0.34$ wt%	
Ilmenite	Subhedral	Groundmass	≤1.6	MgO = 0.1-0.6 wt%	Chromite-Rutile exsolution. Cross-cuts Px and occasionally Plagioclase. Contains glass blebs (≤0.15 mm) exhibiting immiscibility textures and≤ 0.005 mm FeNi metal
Ulvöspinel	Anhedral	Groundmass	≤0.05	MgO = <0.5 wt%	Also as rinds on Chromite
Chromite	Subhedral	Inclusions in Px phenos.	≤0.01	MgO = < 2.5 wt%	
Troilite	Anhedral	Groundmass	≤0.15	---	Associated with ilmenite. Rarely contains FeNi metal blebs
FeNi Metal	Anhedral	Groundmass	<0.01	Co = 1.0-1.5 wt%	Minor interstitial phases
				Ni = 1.2-2.0 wt%	

12061,6 (Fig. 2c)

MINERAL	MORPHOLOGY	RELATIONSHIP	SIZE (MM)	COMPOSITION	SPECIAL FEATURES
Olivine	Anhedral/Embayed	Phenocrysts	≤0.8	Cores = Fo_{60-66}	Some phenocrysts have 0.001 mm glassy rind
		Cores to Px Phenos.	≤0.1	Rims = Fo_{30-35}	
Pyroxene	Subhedral	Phenocrysts	≤1.8	$Wo_{24}En_{50}Fs_{26}$	Phenocrysts have 0.05 mm rind of interwoven
	Anhedral	Groundmass	≤0.5	$Wo_{39}En_{42}Fs_{19}$	glass and olivine
				$Wo_{32}En_{8}Fs_{60}$	
Plagioclase	Subhedral	Groundmass	≤1.0 long	Cores = $An_{89-91}Ab_{11-9}$	Skeletal laths, containing ≤0.05mm inclusions
				Rims = $An_{87-88}Ab_{13-12}$	of Px and glass
Tridymite	Anhedral	Groundmass	≤0.15	---	"Crinkled" Texture
Glass	Interstitial	Groundmass	≤0.2	---	Immiscibility textures
Ilmenite	Subhedral	Groundmass	≤1.0	MgO = 0.3-1.5 wt%	≤0.05 mm rounded glass inclusions.
					Occasional sawtooth margins.
					Elongated prisms
Ulvöspinel	Subhedral	Groundmass	≤0.05	MgO = 0.3-2.0 wt%	Also as rinds on Chromite
				Mg# = 1-6	
				Cr/(Cr+Al) = 0.66-0.74	
Chromite	Anhedral	Inclusions in Px	≤0.001	---	Have Ulvöspinel rinds
Troilite	Anhedral	Groundmass	≤0.05	---	Contains FeNi Metal blebs.
					Occasionally associated with Ilmenite.
FeNi Metal	Anhedral	Groundmass	≤0.1	Co = 1.2-2.3 wt%	Found as blebs in Troilite. Discrete
				Ni = 1.6-6.4 wt%	grains are rare.

12062,12 (Fig. 2d)

No compositions determined due to cover slip on thin section.

MINERAL	MORPHOLOGY	RELATIONSHIP	SIZE (MM)	COMPOSITION	SPECIAL FEATURES
Pyroxene	Subhedral	Groundmass	≤1.5	---	Simple twins on {100}, prismatic crystals
Plagioclase	Subhedral	Groundmass	≤1.2	---	
Tridymite	Anhedral	Groundmass	≤0.3	---	"Crinkled" texture
Glass	Anhedral	Interstitial	≤0.05	---	Opaque
Ilmenite	Subhedral	Groundmass	≤0.8	---	Cross-cut by plagioclase
Ulvöspinel	Anhedral	Groundmass	≤0.15	---	
Chromite	Euhedral	Inclusions in Px	≤0.2	---	
Troilite	Anhedral	Groundmass	≤0.05	---	Occasionally associated with Ilmenite
FeNi Metal	Anhedral	Groundmass	≤0.1	---	Occasionally found as blebs in Troilite

12072,3 (Fig. 2e)

MINERAL	MORPHOLOGY	RELATIONSHIP	SIZE (MM)	COMPOSITION	SPECIAL FEATURES
Olivine	Subhedral	Phenocrysts	≤1.0	Cores = Fo_{70-74}	Contain rounded opaque glass inclusions (≤0.05mm)
				Rims = Fo_{59-67}	Dicontinuous augite overgrowths
Pyroxene	Subhedral/Anhedral	Groundmass	≤0.4	$Wo_9En_{56}Fs_{35}$	Phenocrysts contain resorpotion features
	Subhedral	Phenocrysts	≤1.5	$Wo_{31}En_{42}Fs^{27}$	at edges where glass inclusions are found
				$Wo_{16}En_3Fs_{81}$	
Plagioclase	Subhedral	Phenocrysts	≤0.5	Cores = $An_{91-89}Ab_{9-11}$	Opaque glass inclusuions (<0.1 mm) are
				Rims ≈ $An_{88}Ab_{12}$	present
Tridymite	Anhedral	Groundmass	≤0.2	---	"Crinkled" texture
Glass	Anhedral	Interstitial	≤0.5	SiO_2 = 94-99 wt%	
				FeO = 0.2-3.6 wt%	
				Al_2O_3 = 0.5-0.7 wt%	
Ilmenite	Subhedral	Groundmass	≤0.3	MgO = 0.1-0.25 wt%	Occasional sawtooth margins
Ulvöspinel	Anhedral	Groundmass	≤0.1	MgO < 1 wt%	Also found as rinds on Chromite
Chromite	Subhedral	Microphenocrysts	≤0.5	MgO ≤ 7 wt%	Contains 0.001 mm Ulvöspinel rinds. Found as
					inclusions in outer portions of olivine
					phenocrysts, as well as discrete grains
Troilite	Anhedral	Groundmass	≤0.1	---	
FeNi Metal	Anhedral	Inclusions	≤0.05	Co = 1.3-2.6 wt%	Only found in olivine phenocrysts
				Ni = 2.8-4.6 wt%	

12077,12 (Fig. 2f)

MINERAL	MORPHOLOGY	RELATIONSHIP	SIZE (MM)	COMPOSITION	SPECIAL FEATURES
Olivine	Subhedral	Phenocrysts	≤1.0	Cores = Fo_{70-73} Rims = Fo_{53-67}	Phenocrysts = FeNi Metal inclusions (≤0.02 mm), embayed margins, lack Px overgrowths, contains rounded glass inclusions(≤ 0.3 mm). Forms cores (< 0.5 mm) to larger Px
Pyroxene	Anhedral	Groundmass	≤0.4	$Wo_8En_{62}Fs_{30}$ $Wo_{12}En_{42}Fs_{26}$ $Wo_{18}En_{10}Fs_{72}$	Larger Px contain resorption rinds ≤ 0.1 mm wide containing glass inclusions
Plagioclase	Subhedral	Groundmass	≤0.5 long	Cores = $An_{91-92}Ab_{9-8}$ Rims = $An_{88}Ab_{12}$	Skeletal with Px and Glass inclusions (0.01-0.05 mm)
Glass	Interstitial	Groundmass	0.1-0.2	SiO_2 = 52-60 wt% Al_2O_3 = 14-15 wt% CaO = 12-15 wt% MgO = 0.3-2.2 wt%	
Ilmenite	Subhedral	Groundmass	≤0.7	Mg# = 7-11	Occasional sawtooth margin
Ulvöspinel	Anhedral	Rinds on Chromite	≤0.03	Cr/(Cr+Al) = 0.69-0.73	
Chromite	Euhedral/Subhedral	Groundmass	≤0.3	Mg# = 15-28 Cr/(Cr+Al) = 0.71-0.73	Also found as ≤0.1 mm inclusions in Px, but not Olivine
Troilite	Anhedral	Groundmass	≤0.01	---	Associated with Ilmenite and contains FeNi Metal blebs
FeNi Metal	Anhedral	Groundmass	≤0.02	Co = 1.2-1.6 wt% Ni = 1.6-7.0	Also found as blebs in Troilite and incluions in olivine. Discrete FeNi Metal associated with Chromite-Ulvöspinel.